Pattern Formation in Catalytic Reactors: the Role of Fluid Mixing

P. Arce and D. Ramkrishna
School of Chemical and Engineering, Purdue University, West Lafayette, IN 47907

Fluid-mediated interaction between catalyst particles alone is shown to yield several interesting and significant phenomena in a catalytic reactor that have been generally attributed in the past to direct interaction between particles. Thus, collaborative interaction between particles and the fluid may enhance or abate steady-state multiplicity, and reverse stability behavior. From the simple setting of a population of particles in a well-mixed CSTR, it is shown that the catalyst phase in a catalytic reactor is susceptible to very fine pattern formation in the face of steady-state multiplicity in single particles, which negates the usual assumption that particles exposed to a given fluid have identical states. In a reactor such variability in behavior must be accompanied by a corresponding variability in conversion and selectivity (in multireaction systems) and may have strong implications for reactor control strategies.

Introduction

A recent paper has shown that the commonly used pseudohomogeneous reactor model has serious deficiencies (Ramkrishna and Arce, 1989). It is shown there that the dynamic analysis of "empty" tubular reactors makes essentially incompatible assumptions from the point of view of the more general two-phase, heterogeneous reactor model. Since most dynamic analysis of catalytic reactors in the past has relied on the pseudohomogeneous model, several interesting steady-state and dynamic features of packed reactors have remained unexplored. The two-phase, heterogeneous model clearly represents a more rational model with which dynamic behaviors may be viewed. In this regard, the importance of heterogeneous models has been long recognized by earlier workers (Liu and Amundson, 1962). A very important and interesting attribute of heterogeneous reactor models is recognition of the discrete nature of the catalyst phase. However, that this discrete nature is permissive of a high degree of freedom for the catalyst phase as a whole was a possibility not envisaged by heterogeneous models of the past. It is possible to expect very fine "pattern formation" in the particle phase as a result of multiplicity of stationary states of the catalyst particle and mixing effects in the fluid phase, which a suitably formulated heterogeneous model should be capable of describing. By pattern we imply here that particles exposed to a common fluid environment can assume *different* states, a possibility not generally entertained in reactor models. This issue is not only interesting from a theoretical point of view, but also significant from a practical standpoint since conversion and, even more critically, selectivity in the reactor must depend on the state of the particle phase.

In addressing the issue of patterns, it is essential to recognize the discrete nature of the particle phase. The particles may interact *indirectly* because of mixing in the fluid phase and *directly* because of partial contact between particles. We have recently reviewed several aspects of incorporating these effects in reactor modeling (Arce, 1990). Aside from the work of Schmitz and coworkers (Schmitz and Tsotsis, 1983; Tsotsis, 1983; Brown and Schmitz, 1989), there is virtually no effort in this direction.

This paper focuses on the analysis of indirect interaction of catalyst particles in catalytic reactors. We study an isothermal continuous, stirred-tank reactor (CSTR) with Langmuir-Hinshelwood kinetics. Although a relatively simple model, it is able to show the basic phenomena associated with the formation of patterns that are due to multiple solutions in the individual catalyst particles. In extending this model to a *sequence* of stirred tanks we will have the "cell model" approximation to the packed-bed reactor. Thus the present analysis may be viewed as a precursor to investigating more

Correspondence concerning this article should be addressed to D. Ramkrishna.
The present address of P. Arce is Department of Chemical Engineering, FAMU/FSU College of Engineering, Tallahassee, FL 32516.

detailed models of the packed-bed reactor that account for the discrete nature of the particle phase. Therefore, the study reported in this paper lays the groundwork for investigation of more advanced models within an operator-theoretic framework. We establish here that most of the pathologies attributed usually to direct interaction models (Pismen and Kharkats, 1968) can be achieved in models with indirect interaction only. The relevance of the indirect interaction of the particle phase in reactor analysis was recognized in a study by Luss and Amundson (1968) in the context of fluidized reactors. However, the issue of patterns seems to have been overlooked in their analysis. Our investigation, based on an operator-theoretic approach, has the potential to be generalized to include considerably more complicated models such as the packed-bed reactor within the framework of particle interactions. We present necessary and sufficient conditions for the existence of patterns as well as of *uniform* solutions, that is, the case where all particles have the *same* state. A linearized stability analysis is also reported with very general conclusions for reactors displaying an arbitrary number of particles, N, in the catalyst phase. The analysis also shows the importance of indirect interaction between catalyst particles (due to mass transfer) to produce symmetry breaking of uniform solutions. This fact has not been reported in previous studies (Mankin and Hudson, 1986).

Formulation of the Model

The reactor model can be derived from the general conservation equations, introducing the following assumptions:

1. We neglect thermal effects (isothermal reactor).
2. We assume a well-mixed (reactant) fluid.
3. The reactor is heterogeneous, that is, we distinguish two phases: the fluid phase and the solid phase; the solid phase is viewed as an assemblage of discrete catalyst particles showing the same size, no internal gradients, spherical geometry, and the same active catalyst.
4. The members of the assemblage are assumed to have negligible direct contact between particle neighbors; by contrast, all interaction between the individual catalyst particles takes place *only* through the mixing effects of the fluid.
5. Solid particles are allowed to have different initial conditions.
6. The mass transfer coefficient is assumed to be the same for all particles and the physical properties are constants.

Many of the foregoing hypotheses are standard assumptions made in treating, for example, a laboratory reactor used to determine transport and reaction parameters. The difference lies in the introduction of terms reflecting the possibility of patterns. The formation of patterns has its origin in multiple solutions for catalyst particles. Our analysis will be confined to isothermal situations in which nonlinear kinetics leads to multiplicity. This restriction is not necessary for the analysis (because we are dealing only with ordinary differential equations) but is useful in order to focus more on aspects of pattern formation than on the generality of nonisothermal systems.

With these assumptions, the mass conservation equation for a fluid in a CSTR is:

$$V_f \frac{dc_f}{dt'} = F(c_o - c_f) - \sum_{j=1}^{N} k_m a_p (c_f - c_j) \qquad (1)$$

The mass balance for the jth catalyst particle in the assemblage is:

$$V_p \frac{dc_j}{dt'} = k_m a_p (c_f - c_j) - V_p r'(c_j) \; ; \quad j = 1, 2, \ldots, N \qquad (2)$$

All the symbols used in the model are defined in the Notation. Suitable initial conditions must be added to Eqs. 1 and 2. We may assume for the reaction term, $r'(c_j)$, either linear kinetics (first-order reaction) or nonlinear reaction kinetics. In the latter case, for the purposes of illustration, we will use a Langmuir-Hinshelwood catalytic reaction (Hegedus et al., 1977). However, calculations may be performed with any other suitable kinetics for the system such as, for example, the immobilized enzyme with substrate-inhibited reaction kinetics (DeVera and Varma, 1979). For our particular choice of Langmuir-Hinshelwood catalytic reaction, the mathematical expression for $r'(c_j)$ is given by

$$r'(c_j) = \frac{k(T)c_j}{(1 + \sigma c_j)^2}. \qquad (3)$$

By defining the following nondimensional quantities,

$$Da \equiv \frac{Vk(T)\epsilon}{F(1+\sigma')^2}, \; t \equiv \frac{t'}{\theta_f}, \; x_j \equiv \frac{c_j}{c_o}, \; x_f \equiv \frac{c_f}{c_o}$$

$$\theta_f \equiv \frac{V\epsilon}{F}, \; \alpha_f \equiv \frac{k_m a_p \theta_f}{V\epsilon}, \; \alpha_p \equiv \frac{\theta_f k_m a_p}{V_p}$$

the model may be turned into nondimensional variables. The mathematical model is given by:

$$\frac{dx_f}{dt} = (1 - x_f) - \alpha_f \sum_{j=1}^{N} (x_f - x_j) \qquad (4)$$

$$\frac{dx_j}{dt} = \alpha_p (x_f - x_j) - r(x_j), \; j = 1, 2, \ldots, N \qquad (5)$$

The reaction kinetics, $r(x_j)$, may assume either the following linear reaction rate

$$r(x_j) = \phi^2 x_j \qquad (6)$$

where ϕ^2 is the standard Thiele modulus, or the following nonlinear reaction rate, which is Eq. 3 conveniently nondimensionalized:

$$r(x_j) = Da\, f(x_j) = Da \frac{(1 + \sigma')^2 x_j}{(1 + \sigma' x_j)^2} \qquad (7)$$

First-Order Reactions

In this section we discuss the linear case of the reactor model; that is, we consider first-order reaction kinetics. This section is important for the operator formulation of the model and

for relating the extent of indirect interaction to the spectrum (eigenvalues) of the operator. The spectral properties of this operator are also of significance to the stability analysis of steady states to follow.

Operator formulation

Since we have a two-phase system, it is convenient to define two Hilbert spaces associated with each phase in the problem. Let H_p be the Hilbert space of the catalyst particle phase and H_f be that for the fluid phase. Then the following direct sum Hilbert space, H (see Ramkrishna and Amundson, 1985, for a definition of *direct sum*), is the space associated with the reactor operator L_N, defined in Eq. 11 below.

$$H \equiv H_f \oplus H_p \tag{8}$$

Any vector $x \epsilon H$ will have the form

$$x^T \equiv (x_f\,;\, x_N) = (x_f\,;\, x_1, x_2, \ldots, x_N)$$

where $x_f \epsilon H_f$ and $x_N \epsilon H_p$. The index f refers to the fluid and is not an integer. (Because the fluid phase is described by a *simple* concentration, the Hilbert space H_f is the set of real numbers only. For more complicated models such as a sequence of m stirred tanks H_f will be R^m, the space of m-dimensional vectors. H_p is clearly R^N.) The boldface symbol x_N is to be distinguished from its component x_N. Now we define the following operators:

The fluid operator F such as

$$F\colon H_f \to R;\ x_f \to (1 + N\alpha_f)x_f \equiv \mu_N x_f$$

The *solid-fluid interaction operator* A:

$$A\colon H_p \to R;\ A = -\alpha_f \mathbf{1}_N\cdot$$

where $\mathbf{1}_N^T \equiv [1, 1, \ldots 1] \epsilon H_p$ and the dot refers to forming the regular inner product with the vector in H_p on which A acts.

The *particle phase operator* S_N:

$$S_N\colon H \to H_p;\ S_N \equiv \nu I_N$$

where I_N is the unity operator on H_p, $\nu \equiv \alpha_p + \phi^2$.

The *fluid-solid interaction operator* B:

$$B\colon R \to H_p\colon B(1) = -\alpha_p \mathbf{1}_N$$

The action of B on any number, say β, produces the vector $-\alpha_p\beta\mathbf{1}_N \epsilon H_p$.

By defining the following perturbation variables, with respect to the steady state x^∞, $\hat{x}_N = x_N - x_N^\infty$ and $\hat{x}_f = x_f - x_f^\infty$, we may write the reactor problem given by Eqs. 4, 5, and 6 in the following way.

$$-\frac{d\hat{x}}{dt} = \mathbf{L}_N\hat{x} \tag{9}$$

with the following initial condition

$$\hat{x}(t=0) = \hat{x}_o \tag{10}$$

The matrix *reactor operator* L_N is defined as follows.

$$L_N \equiv \begin{bmatrix} F & A \\ B & S_N \end{bmatrix} \tag{11}$$

where the elements of the $(N \times N)$ diagonal matrix particle phase operator S_N are given by its eigenvalues $(\alpha_j + \phi^2)$. In the general case, the elements of the vector of initial conditions, x^o, will not be equal to each other (i.e., $x_1 \neq x_2 \neq \ldots \neq x_N \neq x_f$). We will refer to this initial condition as being *nonuniform*.

Inner Product. Let $w_j, j = 1,2$ be two elements of the Hilbert space H:

$$w_j = \begin{bmatrix} u_j \\ v_j \end{bmatrix},\ j = 1, 2$$

Then the following inner product may be defined for this direct sum Hilbert space:

$$\langle w_1, w_2 \rangle \equiv u_1 u_2 + \delta(v_1, v_2)_p \tag{12}$$

where δ is a constant to be determined to make the reactor operator L_N self-adjoint in the Hilbert space H. The inner product $(\ ,\ )_p$ in the particle Hilbert space, H_p, may be chosen as the Euclidean inner product. $(v_j, v_k)_p \equiv v_j \cdot v_k$.

Self-adjoint Condition for L_N. By using the inner product given by Eq. 12, it is not difficult to obtain:

$$\langle L_N w_1, w_2 \rangle - \langle w_1, L_N w_2 \rangle$$

$$= (\alpha_f - \alpha_p\delta)[(\mathbf{1}_N u_1, v_2)_p - (\mathbf{1}_N u_2, v_1)_p]$$

The condition to make L_N a self-adjoint operator is that the previous equation vanish for arbitrary $w_1, w_2 \epsilon H$. This is possible by seeking $(\alpha_f - \alpha_p\delta) = 0$, which produces the following result: $\delta = \alpha_f/\alpha_p$. Furthermore, the operator L_N is a nonnegative definite operator. This may be shown by computing

$$\langle L_N w, w \rangle = u^2 + \alpha_f \|\mathbf{1}_N u - v\|_p^2 + \delta\phi^2 \|v\|_p^2$$

which clearly is greater than or equal to zero for arbitrary $w \epsilon H$. Furthermore, the spectral theorem (Ramkrishna and Amundson, 1985) assures us that the eigenvalues of L_N are *real-valued* and the corresponding set of eigenvectors is *complete*. Also, eigenvectors belonging to different eigenvalues are orthogonal with respect to the inner product, Eq. 12. Finally, since L_N is a nonnegative definite operator, the nonzero eigenvalues are all positive.

Eigenvalue problem

The eigenvalue problem for the operator L_N may be written as

$$L_N w = \lambda w$$

This problem yields the equation

$$\left[\frac{-\alpha_p\alpha_f}{(\mu_N-\lambda)}\,(\mathbf{1}_N \otimes \mathbf{1}_N) + (S_N - \lambda I_N)\right]v = 0 \qquad (13)$$

where we have used the tensor product notation $\mathbf{1}_N \otimes \mathbf{1}_N$ merely to represent an $N \times N$ matrix whose elements are all unity. The characteristic equation is given by

$$p_N(\lambda) \equiv (\nu-\lambda)^{N-1}\,[(\nu-\lambda)\,(\mu_N-\lambda) - N\alpha_f\alpha_p] = 0 \qquad (14)$$

This characteristic equation has interesting properties. We have a multiple root (for $N \geq 3$) which is given by the eigenvalue of the "isolated" particle operator

$$\lambda_j = \nu = \alpha_p + \phi^2, \quad j = 2, 3, \ldots, N \qquad (15)$$

We also have *two* more roots that are produced by equating the square bracket term of Eq. 14 to zero. This is a quadratic equation that admits the following solutions:

$$\lambda_j = \frac{\nu+\mu_N}{2} \pm \frac{1}{2}\,[\nu^2 + \mu_N^2 - 2\nu\,\mu_N + 4N\alpha_f\alpha_p]^{1/2}\,,$$

$$j = 1 \text{ and } N+1 \qquad (16)$$

We have assigned j to take values so that the eigenvalues $\{\lambda_j\}$ are in increasing order. The quadratic equation yields the smallest and the largest eigenvalue of the operator L_N. All the other λ_j's (given by Eq. 15) are sandwiched between these λ_1 and λ_{N+1}. In order to obtain this shape of the spectrum of L_N we transform the portion of Eq. 14 that yields the quadratic equation, that is, $[\,] \equiv 0$, as follows:

$$\frac{\lambda-\mu_N}{N\alpha_f} = \frac{\alpha_p}{\lambda-\nu} \qquad (17)$$

Setting

$$\Phi(\lambda) \equiv \frac{\lambda-\mu_N}{N\alpha_f} \qquad (18a)$$

$$\Sigma(\lambda) \equiv \frac{\alpha_p}{\lambda-\nu} \qquad (18b)$$

We note that the eigenvalues of L_N (corresponding to the quadratic portion of the characteristic Eq. 14) occur at the intersection of $\Phi(\lambda)$ and $\Sigma(\lambda)$. This function displays only two branches: $\Sigma_1(\lambda)$ to the left of the singularity ($\lambda = \nu = \alpha_p + \phi^2$), and $\Sigma_2(\lambda)$ to the right of this singular point. The singularity of $\Sigma(\lambda)$ becomes an eigenvalue for $N=2$, and it becomes a *multiple* eigenvalue for $N \geq 3$. A geometrical view of the spectrum of L_N is shown in Figure 1. The two eigenvalues yielded by the quadratic equation (λ_1, λ_{N+1}) are the two eigenvalues associated with the two-phase, heterogeneous reactor model without indirect interaction between the catalyst particles (Do and Rice, 1985).

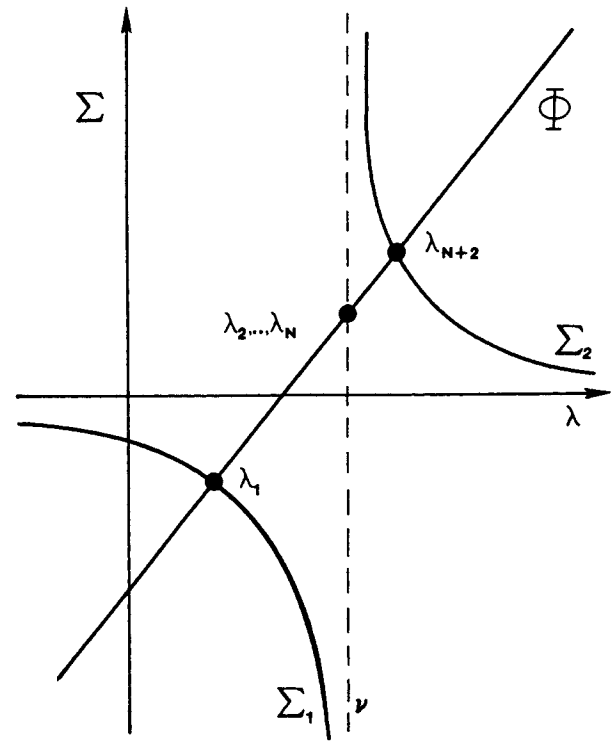

Figure 1. Geometrical view of spectrum of L_N for first-order reactions.

Expansion of the initial conditions

The solution to Eq. 9, in terms of eigenvalues and eigenvectors of L_N, is given by

$$\hat{x}(t) = \sum_{j=1}^{N+1} \langle x^0, w_j\rangle e^{\lambda_j t} w_j \qquad (19)$$

where the expansion coefficients, $\langle x^0, w_j\rangle$, are given by the inner product, Eq. 12. The $w_j (j=1, 2, \ldots, N+1)$ are the eigenvectors of L_N. These can be readily computed as

$$w_j = c_j\left[\frac{1}{\alpha_p}{(\nu - \lambda_j)}\,\mathbf{1}_N\right], \quad j = 1 \text{ and } N+1$$

where $\mathbf{1}_N \epsilon H_p$ has all its elements to unity, and the c_j is the jth normalization coefficient given by

$$c_j = \frac{1}{\left[1 + \dfrac{\alpha_f\alpha_p N}{(\nu-\lambda_j)^2}\right]^{1/2}}, \quad j = 1 \text{ and } (N+1).$$

Since L_N is self-adjoint, the multiplicity of the eigenvalue ($\alpha_p + \phi^2$) is also the dimension of the corresponding eigenspace. Thus there are $(N-1)$ eigenvectors w_j corresponding to the eigenvalue $\lambda_j = (\alpha_p + \phi^2)$, $j = 2, 3, \ldots, N$ given by

$$w_N = c_N \begin{bmatrix} 0 \\ \mathbf{1}_{N-1} \\ -(N-1) \end{bmatrix}, \quad w_{N-1} = c_{N-1} \begin{bmatrix} 0 \\ \mathbf{1}_{N-2} \\ -(N-2) \\ 0 \end{bmatrix}, \quad \ldots, \quad w_2 = c_2 \begin{bmatrix} 0 \\ 1 \\ -1 \\ \mathbf{0}_{N-2} \end{bmatrix}$$

where the normalization constants are given by:

$$c_N = \frac{1}{[(N-1)\delta + (N-1)^2\delta]^{1/2}},$$

$$c_{N-1} = \frac{1}{[(N-2)\delta + (N-2)^2\delta]^{1/2}}, \ldots, c_2 = \frac{1}{(2\delta)^{1/2}}$$

If we let the initial concentration vector x^0 in Eq. 9 be orthogonal to the eigenspace corresponding to the eigenvalue $\alpha_p + \phi^2$, then we may write

$$\langle x^o, w_j \rangle \equiv 0, \quad j = 2, 3, \ldots, N. \tag{20}$$

It is easy to see that the only vector x^o consistent with Eq. 20 has all components equal, which corresponds to the situation where all the particles of the assemblage have the same concentration (the uniform initial condition). From Eq. 19 it follows that if x^o satisfies Eq. 20, $\hat{x}(t)$ also satisfies Eq. 20 at all times. Thus if all the particles have initially the same concentration they retain this uniformity at all times. (That this is also true of the nonlinear case can be established relatively easily). Alternatively, we reach the important conclusion that a pattern (of nonidentical concentrations) is associated with initial concentration vectors containing components in the space spanned by $w_j, j = 2, 3, \ldots, N$. The reactor model discussed in this paper *a priori* admits this class of initial conditions. Other limiting cases may be derived following a strategy similar to the one previously published by Arce and Ramkrishna (1986) and Ramkrishna and Arce (1988, 1989). We prefer here to discuss the issues related to nonlinear kinetics and those associated with pattern formation.

Nonlinear Kinetics: Steady State Analysis

In this section we discuss the issues related to the stationary solutions of the indirect interaction reactor model when we have nonlinear reaction kinetics. We will be concerned with the steady state solutions of the reactor containing an arbitrary number N of particles; such steady states will include both uniform (patternless) solutions, and patterned solutions. More specifically, it will be of interest to establish conditions under which uniform or patterned solutions will manifest. We will illustrate the results of our analysis with examples of reactors containing a few catalyst particles in the system. However, we will also address how the situation would change when the system displays a larger number of catalyst particles.

Steady state of the assemblage

We begin by obtaining the steady state equation for the model of Eqs. 4 and 5. If we drop the time derivative of these two equations we obtain:

$$\frac{1}{\alpha_f}(1 - x_f) = \sum_{j=1}^{N} (x_f - x_j) \tag{21}$$

$$\frac{\alpha_p}{Da}(x_f - x_j) = f(x_j), \quad j = 1, 2, \ldots, N \tag{22}$$

where $f(x_j)$ is the Langmuir-Hinshelwood kinetics given by Eq. 7. Equation 21 may be transformed to yield the following relation:

$$-\frac{1}{\alpha_f} + \left[N + \frac{1}{\alpha_f}\right] x_f = \sum_{j=1}^{N} x_j$$

By defining the following two functions

$$D(x_f) \equiv -\frac{1}{N\alpha_f} + \left[1 + \frac{1}{N\alpha_f}\right] x_f \tag{23}$$

$$\bar{X}_N^k(x_f) \equiv \frac{1}{N}\sum_{j=1}^{N} x_j, \quad k = 1, 2, \ldots, M_m \tag{24}$$

the steady state equation of the model may be written as follows

$$D(x_f) = \bar{X}_N^k(x_f), \quad k = 1, 2, \ldots, M_m \tag{25}$$

The reactor steady states are located graphically from the intersections of $D(x_f)$ and $\bar{X}_N^k(x_f)$ plotted vs. x_f. In Eq. 24, M_m represents the number of *distinct* combinations of catalyst particle states that influence the fluid-phase concentration; it must clearly depend on m, the number of steady states possible for the isolated particle. It must be borne in mind that there are many more than M_m combinations of actual catalyst particle states but they need not all be considered because the fluid phase does not distinguish between particles of the same state. This is an aspect of the inherent symmetry of the system that makes possible the application of group-theoretic methods in the analysis of this problem. However, we defer such features to a later paper. The value of M_m can be shown using combinatorial arguments to be

$$M_m = \frac{(N+1)(N+2)\ldots(N+m-1)}{(m-1)!} \tag{26}$$

Equation 24 represents M_m curves, which we shall refer to as branches. The reactor steady states are obtained by the intersection of the line, Eq. 23, with the family of curves, Eq. 24. For example, for a reactor with two particles ($N=2$) with three possible steady states for each (i.e., $m=3$), Eq. 26 yields six branches of curves in the family of Eq. 24. For three particles

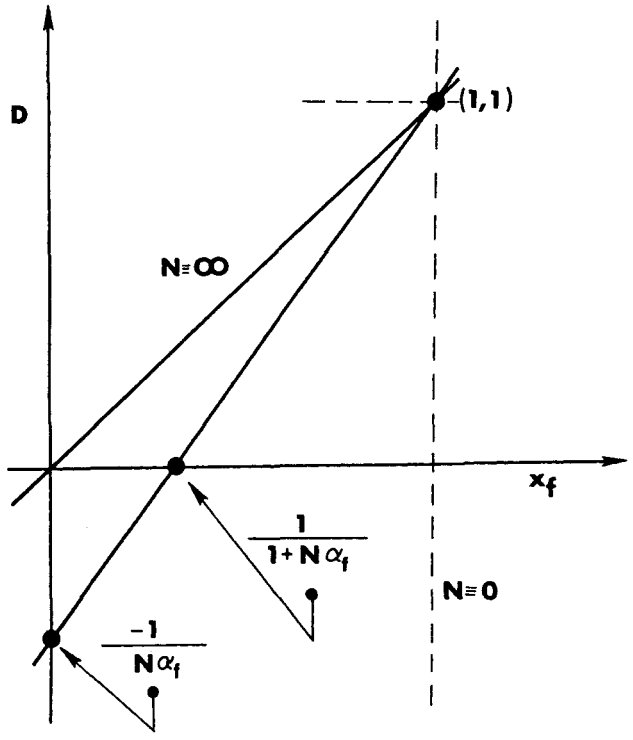

Figure 2. Shape of function $D(x_f)$.

the maximum number of branches from Eq. 26 is ten; Figure 4.

The main features of the function $D(x_f)$ are shown in Figure 2. Clearly, it is a straight line with a positive slope given by $(1+1/N\alpha_f)$. It has a pivoting point at (1,1) and it has two asymptotic lines: a 45° line (for $N = \infty$) and a vertical line ($N \equiv 0$) passing through the pivoting point (1,1). These two asymptotes jointly with the axis $D(x_f) = 0$ define a triangular region that is the domain of feasible steady state solutions to Eq. 25.

Since the function $\bar{X}_N^k(x_f)$ is computed from the concentration values (x_j) associated with the individual particles, it is convenient to study the mass balance of the jth particle, which is given by Eq. 22. This equation may be rearranged to give

$$x_f = G(x_j), \quad 0 = 1, 2, \ldots, N$$

where $G(x_f) \equiv x_j + (Da/\alpha_p)f(x_j)$. The equation written before may be solved (inverted) for any fixed value of $x_f \in (0, 1)$. Let us denote this procedure by $X(x_f) = G^{-1}(x_f)$. It is useful to distinguish two possible graphs of the function $X(x_f)$ as they are shown in Figures 3a, b. The shape of $X(x_f)$ displayed in Figure 3a is a single-valued function of x_f. In this case the catalyst particle (in "isolation") is able to show only one concentration value, x_j, for any given value of the concentration of the fluid, x_f^*. The case shown in Figure 3b corresponds to a multivalued function $X(x_f)$ for a certain range of the concentration of the fluid $(x_f, \bar{x}_f)$. We let $\bar{x}_p$ be the particle state in fluid of concentration x_f, and x_p be the particle state in fluid of concentration $\bar{x}_f$. It is the circumstances in Figure 3b that provide for the possibility of patterns. Interestingly, Eq. 24 merely calculates (for each x_f) an arithmetic average of the different particle steady states.

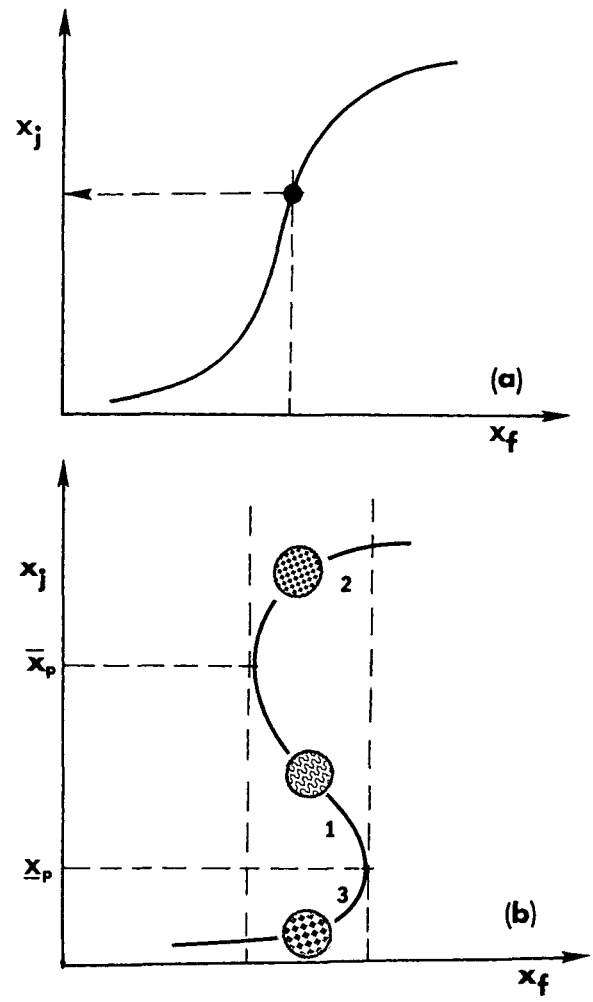

Figure 3. Graphs of function $X(x_f)$.

It is clear, now, that the portrait shown in Figure 3a can only display uniform steady states since a particle can only have a single steady state for each x_f. In this case we obtain $\bar{X}_N^k(x_f) \equiv X(x_f)$, which implies that the graph of the function, Eq. 24, is given by the graph of $X(x_f)$ itself.

Examples. For illustration of the case of Figure 3b we present calculations for three particles (the number of particles places no severe burden either on analysis or computation) in which the particle states are tagged 1, 2, and 3 distinguished by different pattern symbols as shown. The physical and kinetic parameters in these calculations are chosen to be realizable in an experimental reactor such as Carberry reactor. For three particles Eq. 26 yields the number of branches as ten. Table 1 presents the number of particles N_1, N_2, and N_3 with steady states 1, 2, and 3, respectively. Figure 4 shows the same information with pattern symbols. Beside the uniform states (1, 4, and 10), we also have seven nonuniform configurations. Figure 5 shows the calculation of $\bar{X}_N^k(x_f)$ $(k = 1, 2, \ldots, 10)$ from Eq. 24. We use dashed lines (2, 3; 5-9) to indicate the nonuniform branches and continuous lines (1, 4, and 10) to show the uniform stationary branches. As observed earlier, the steady states of the model will occur at the intersection of the line $D(x_f)$ with $\bar{X}_3^k(x_f)$, $k = 1, 2, \ldots 10$. For example Figure 5 illustrates two possible cases of stationary solutions

Table 1. Configuration of Reactor States for the Three-Particle Problem

N_1	N_2	N_3	$\bar{X}_3^k$
0	0	3	1
1	0	2	2
2	0	1	3
3	0	0	4
0	1	2	5
1	1	1	6
2	1	0	7
0	2	1	8
1	2	0	9
0	3	0	10

for the ratio $Da/\alpha_p = 0.048$: The function $D(x_f)$ with $\alpha_f = 1/3$ shows *only* one steady state (branch 10, a uniform stationary state), but for $\alpha_f = 1/2$ branches 1, 2, 3, 4, and 10 yield *five* steady states. Note that branches 2 and 3 are nonuniform while 1, 4 and 10 are uniform configurations. In a later section stability analysis is performed to determine which one of these solutions is stable. By following a procedure similar to the case $N=3$ we can compute the function $\bar{X}_N^k(x_f)$ ($k = 1, 2, \ldots, M_m$) for any arbitrary number of particles in the reactor model. The *three* uniform branches are obtained for any number N of particles. However, the number of nonuniform branches will increase considerably ($M_m - 3$) as we increase the number of particles in the assemblage. This fact implies that the number of dashed lines—of, for example, Figure 5 —will increase (as N increases), packing the space between the lower and upper uniform stationary branches. From this representation, it is clear that small perturbations of the steady states should be enough for the reactor to change from one state to another. As the number of particles increases the intercept of $D(x_f)$ on the D axis changes from $-[1/(N\alpha_f)]$ to zero. Thus all possible solutions will be located in the feasible region defined by the triangular region with sides given by asymptotes $N \equiv \infty$ and $N \equiv 0$, and the axis $D(x_f) \equiv 0$.

In the following sections we discuss some general conditions governing the steady state structure of the system for an arbitrary number of particles.

Uniqueness conditions for uniform states

In this section we present the necessary and sufficient conditions under which a unique uniform (or, alternatively, patternless) solution exists. The result is obtained by a simple extension of the analysis reported by Luss (1971) for the case of single-particle analysis and homogeneous CSTR. Following Luss we define the function $F(x)$ by

$$F(x) \equiv \frac{f(x)}{(1-x)}$$

the uniqueness condition is expressed by either of the conditions

$$M_a < F(\bar{x}) \ , \ M_a > F(\underline{x}) \qquad (27)$$

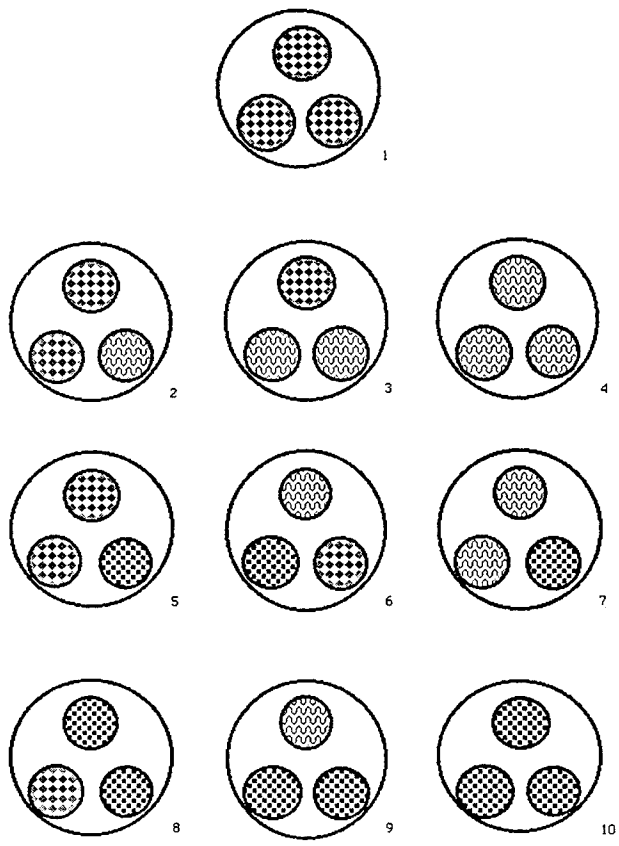

Figure 4. Configurations of stationary states for $N=3$.

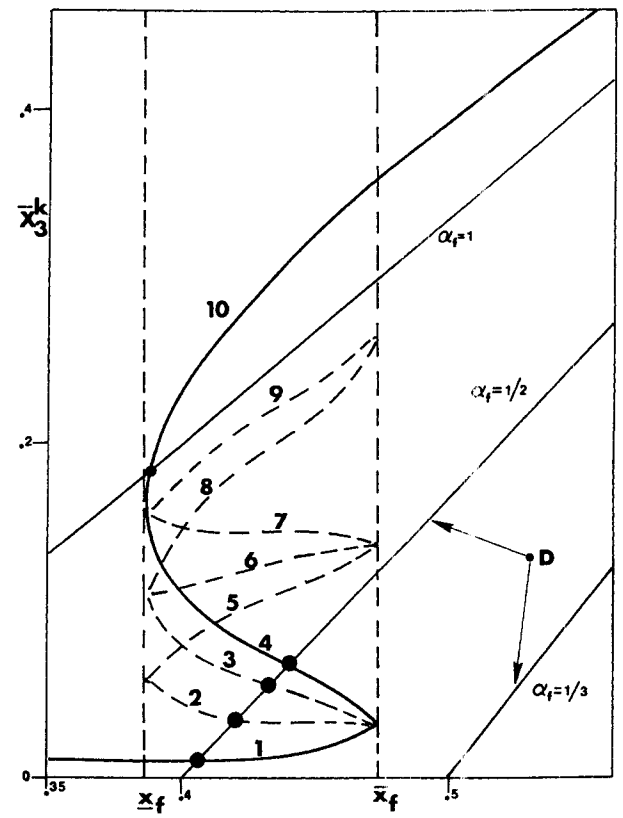

Figure 5. Steady state structure of model for three-particle system.

$Da/\alpha_p = 0.048$, $\alpha_f = 1/3$, $\alpha_f = 1/2$

where $\underline{x}$ and $\bar{x}$ are the roots of $F'(x)=0$ given by

$$\underline{x} = \frac{1}{4}\left(1 - \sqrt{1 - \frac{8}{\sigma'}}\right), \quad \bar{x} = \frac{1}{4}\left(1 + \sqrt{1 - \frac{8}{\sigma'}}\right)$$

and the parameter M_a is defined by

$$M_a \equiv \frac{\alpha_p}{Da(1 + \alpha_f N)} = \frac{M_p}{(1 + \alpha_f N)}$$

Conversely *multiple uniform* solutions exist *if and only if*

$$F(\bar{x}) \leq M_a \leq F(\underline{x}) \tag{28}$$

Note that under this condition, Eq. 28, *patterned solutions may* also coexist although it is not necessary that they do so. However, the issue of patterned solutions will be discussed more fully in the next section. For the present we illustrate the consequences of the conditions of Eqs. 27 and 28.

The effect of the number of particles N on the behavior of the assemblage is better illustrated in Figure 6. In this figure the isolated particle shows only unique solutions (for each concentration x_f of the fluid, as for example in Figure 3a) but the assemblage displays a variety of behaviors. For example, where $N = 1$ and $N = 19$ the collection of particles shows unique solutions. However, for $N = 5$ the assemblage interestingly shows multiple solutions while the isolated particle only displays unique steady states. Note that while an increase from 1 to 5 in the number of particles has promoted multiplicity, a further increase from 5 to 19 has eliminated multiplicity. The foregoing considerations should dispel a prevalent notion (although not often expressed) that if the catalyst particles in a reactor have unique steady states the reactor should also have a unique steady state. Figure 5 shows the circumstances for the assemblage when the single particle exhibits multiplicity, Figure 3b. For three particles, branches corresponding to patterns have been identified in Figure 5. Varying α_f from a value of 1/3 at which a unique steady state is exhibited by the assembly, multiple uniform *and* patterned steady states totaling five (the fifth not in range in the figure) are obtained at $\alpha_f = 1/2$, while $\alpha_f = 1$ produces only multiple uniform steady states. Clearly, further increase in α_f would produce a unique steady state in the assembly. Again the above instances dispel the viewpoint that multiplicity in catalyst particles should promote multiplicity in the reactor. Another interesting point to be made is that when multiplicity occurs in the assembly with patterns, there is a maximum of three uniform steady states, sometimes with two lying along the same branch of uniform solutions (such as 1 or 10 in Figure 5). This occurs when the particle steady state is between $\bar{x}$ and $\bar{x}_p$ or between $\underline{x}$ and $\underline{x}_p$.

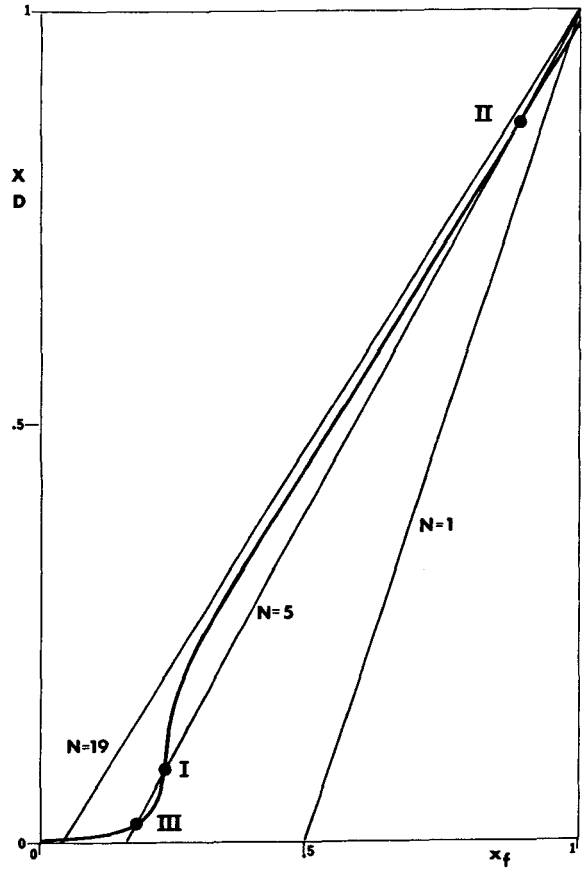

Figure 6. Reactor multiplicity when all particles in isolation show uniqueness of steady states.

Conditions for the existence of patterns

In the previous section we established necessary and sufficient conditions, Eq. 27, for a unique steady state of the system. When the above conditions are violated multiple solutions must exist. Such multiplicity may provide for either uniform solutions or patterned solutions. In Figure 4 we have seen a diverse variety of patterns numbering seven for the three-particle assembly. We seek to determine conditions under which each of the above patterns may come to exist. Recall that the patterns are recognized by dashed curves in Figure 5, which are obtained by summing integral multiples N_1, N_2, N_3 respectively, as shown in Figure 3b or from the expression in Eq. 24. The strategy for the existence of patterns follows very much that of the existence of uniform solutions in that a substitute must be found for the function $F(x)$ used for the latter. For the kth pattern in an N-particle assembly we define the function (following Eq. 25).

$$F^k(x_f) \equiv \frac{x_f - \bar{X}^k_N(x_f)}{1 - x_f} \tag{29}$$

Since the steady state for the kth pattern is obtained at the intersection of the curve of Eq. 29 with $[1/(\alpha_f N)]$, we obtain the following criterion for the existence of the kth pattern

$$F^k(\underline{x}_f) \leq \frac{1}{\alpha_f N} \leq F^k(\bar{x}_f) \tag{30}$$

Condition 30, which was obtained by recognizing that the values of $F^k(x_f)$ must lie between its value at $\underline{x}_f$ and $\bar{x}_f$, is in fact the *necessary and sufficient condition* for the kth pattern provided it is *strictly monotone* in the range between $\underline{x}_f$ and

$\bar{x}_f$. If, however, the kth pattern has an interior extremum represented by the condition

$$\frac{dF^k}{dx_f}(x_f) = 0 \tag{31}$$

for some x_f, condition 31 leads to

$$\frac{\mu_N}{\alpha_f} = \frac{N_2}{1 + \dfrac{f'(x^{(2)})}{M_p}} + \frac{N_3}{1 + \dfrac{f'(x^{(3)})}{M_p}} \tag{32}$$

which follows from Eq. 29. Note that Eq. 32 does not contain a term for steady state 1 because $N_1 = 0$. Condition 31 or 32 is realized at two points $\underline{x}_f^k$ and $\bar{x}_f^k$ (the superscript signifying a branch k of the assembly) at which the line representing $D(x_f)$ is exactly tangential to the curve $\bar{X}_N^k(x_f)$. Now if the kth pattern satisfies condition 31, condition 30 becomes only a *sufficient* condition for its existence. This sufficiency can be further improved by the *necessary* and *sufficient* condition for the existence of the kth branch given by

$$F^k(\underline{x}_f^k) \le \frac{1}{\alpha_f N} \le F^k(\bar{x}_f^k) \tag{33}$$

A particularly interesting fact to observe is that when Eq. 31 is not satisfied the kth branch will have a *unique* representative. On the other hand, when Eq. 31 is true, multiplicity develops on this branch itself. Thus there are *two* solutions for this pattern branch. (Note that each branch lies strictly between $\underline{x}_f$ and $\bar{x}_f$, terminating at those end points except for the uppermost branch, which extends beyond $\bar{x}_f$, and the lowermost branch, which extends to the left of $\underline{x}_f$.) The range in Eq. 33 for the parameter $[1/(\alpha_f N)]$ can be further narrowed to identify the region of multiplicity on this branch. The result is either of the following

$$F^k(\underline{x}_f^k) \le \frac{1}{\alpha_f N} \le F^k(\underline{x}_f)$$

$$\tag{34}$$

$$F^k(\bar{x}_f) \le \frac{1}{\alpha_f N} \le F^k(\bar{x}_f^k)$$

Figures 5 and 7 provide a demonstration of the different circumstances under which the kth pattern will manifest. For a three-particle assembly with $\sigma' = 35$, $M_p = 11.8$, inequality 30 becomes $0.3944 \le \alpha_f \le 0.6179$. In Figure 5 we clearly encounter for $\alpha_f = 1/3$ both a violation of condition 30, and the absence of the pattern for $k = 2$. On the other hand, for $\alpha_f = 1/2$, condition (30) is satisfied for $k = 2$ and the existence of the kth pattern is confirmed in Figure 5. Figure 7 is concerned with a two-particle assembly and the existence of the branch marked as 4 for which condition 31 holds. Inequality 33 then becomes $0.889 \le \alpha_f \le 0.956$. Thus for $\alpha_f = 1$, it follows from Eq. 33 that the kth branch does exist, which is confirmed by Figure 7. Furthermore, $\alpha_f = 1$ satisfies one of the conditions, Eq. 34, so that *two* solutions must exist for this pattern, which also follows from Figure 7.

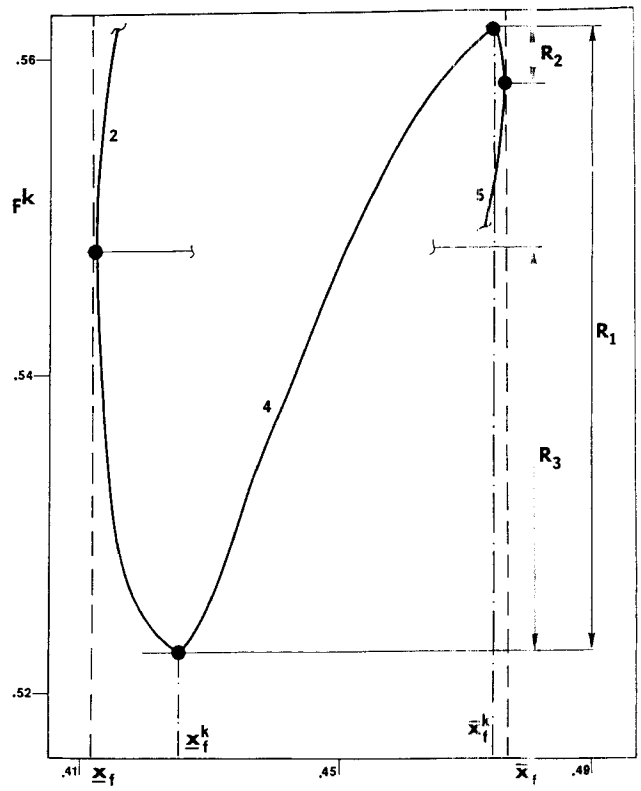

Figure 7. Multiplicity ranges of $(\alpha_f N)$ for pattern with particles at lower and upper steady states when $N = 2$.

R_1: range for existence of branch 4. R_2, R_3: ranges where multiplicity of branch 4 is possible

Clearly, it is now possible to state the condition for *any* of the $(M_m - 3)$ patterned solutions to exist as

$$\min_{k\in\{2,3,\ldots,M_m-3\}} F^k(\underline{x}_f) \le \frac{1}{\alpha_f N} \le \max_{k\in\{2,3,\ldots,M_m-3\}} F^k(\bar{x}_f) \tag{35}$$

If the patterns are numbered in a particular way—such as, for example, $k = 2$ for the lowest branch, $k = M_m - 3$ for the highest branch, Figure 5, (the numbering of branches in between the lowest and the highest branch is done *arbitrarily*) — the left end of inequality Eq. 35 is given by $F^2(\underline{x}_f)$ and the right end is given by $F^{M_m-3}(\bar{x}_f)$. In a three-particle assembly, no patterns can be shown to exist for $\alpha_f = 1/3$ from inequality Eq. 35, a fact also borne out by Figure 5. Note that Eq. 35 is both necessary and sufficient for any patterned solution to exist. This fact is not totally evident at this point and will be elucidated during a discussion of the stability of each branch.

The communication between catalyst particles through the mixing in the reactant fluid (i.e., the indirect interaction mechanism) described in this paper plays a very important role in the behavior of the catalytic reactor. Moreover, the model discussed here displays all the pathologies usually attributed to direct interaction between particles. Two additional facts are noteworthy.

First, the particle assembly can display multiplicity with fluid environments in which the isolated individual particles will

have only unique steady states. This may be referred to as *collaborative multiplicity,* or more generally *collaborative enhancement* of multiplicity. Second, the assembly may also possess a unique steady state with a fluid environment in which the individual particles in isolation may display multiplicity. This is clearly a situation of *collaborative abatement* of multiplicity.

At this stage of our analysis it is very important to note the relevance of considering the problem of interaction between catalyst particles in its different aspects independently. We believe that the investigation of the indirect interaction alone can be performed for considerably more complicated situations than in the direct-interaction models. Of course, these remarks are not intended to deny the role of any direct interaction that may occur between particles.

The analysis of this paper is based on complete understanding of the steady state picture of the isolated single particle problem. This understanding is reflected in the use of the functions $\bar{X}_N^k(x_f)$ (defined by Eq. 24) in Eq. 25. Equations 25 represent M_m uncoupled equations each of which may or may not have a solution. The derivation of Eq. 25 was made possible because of being constrained to only fluid-mediated interactions between particles. They themselves give rise to individual bifurcation problems that are somewhat similar to the bifurcation problems associated with the single particle. The multiplicity of the reactor, which is the sum of the multiplicities of the M_m Eqs. 25, can be calculated exactly for any parameter values using the conditions given by Eqs. 27, 28, 30, and Eqs. 33–36. Note that the inherent symmetry of the problem was built in *a priori* in arriving at the individual Eqs. 25. An alternative approach lies in deriving the reduced bifurcation equations using group-theoretic methods (Gmitro and Scriven, 1966; Othmer and Scriven, 1971; Sattinger, 1979; Golubitsky et al., 1988), which do not depend on complete prior information on the single-particle problem for an entire range of fluid conditions.

Stability Analysis

In this section we perform a linear stability analysis of the different stationary solutions (i.e., uniform and patterned steady states). The importance of this analysis lies in the fact that it will determine what kind of patterns will develop when a uniform steady state becomes unstable. Alternatively, the linear stability analysis permits us to know the various choices of the systems when symmetry breaking takes place. Among the several nonuniform solutions, the system will choose those patterned states that are stable to small perturbations. The linearized stability analysis of this system is fairly straightforward.

Linearized operator L_N

We consider the system of equations given by Eqs. 4 and 5 together with the reaction rate kinetics given by Eq. 7. For the purposes of derivation only, we will assume that the N catalyst particles are located such that there are N_1 particles corresponding to the steady state "1", N_2 to the steady state "2", and N_3 to the steady state "3". The linearized model equation is written in the same form as Eq. 9. Note that for this form asymptotic stability is governed by *positivity* of the real parts of the eigenvalues. The operator L_N is given by the same matrix of Eq. 11 where all operators have been identified earlier, in the model formulation section. The particle phase operator S_N is a $(N \times N)$ matrix whose diagonal displays the eigenvalues of the single-part operator. These eigenvalues are given by

$$\nu_k \equiv \alpha_p + Daf'(\bar{x}_k), \quad k = 1, 2, 3$$

where the prime denotes the first derivative of the kinetic function, $f(x)$, evaluated at the corresponding steady state ($\bar{x}_k$, $k = 1, 2, 3$). The diagonal terms ν_k ($k = 1, 2, 3$) of S_N in L_N replace $(\alpha_p + \phi^2)$ appearing in the original linear operator for the linear case. The operator L_N is self-adjoint in H under the inner product, Eq. 12. Furthermore, unlike the linear operator, Eq. 11, L_N is an indefinite operator since ν_ks may take positive, negative or zero values. In what follows the eigenvalues of L_N are investigated. Since the operator L_N is self-adjoint the eigenvalues are all real and periodic solutions are prohibited.

As before, let λ be an eigenvalue of L_N and w be the corresponding eigenvector. The eigenvalue problem associated with L_N is given by $L_N w = \lambda w$. This problem yields the following characteristic equation:

$$p_N(\lambda) \equiv \left[\prod_{j=1}^{m} (\nu_j - \lambda)^{(N_j - 1)}\right] \hat{p}_N(\lambda) = 0 \tag{36}$$

where

$$\hat{p}_N(\lambda) \equiv \left[(\mu_N - \lambda) \prod_{j=1}^{m} (\nu_j - \lambda) - \alpha_f \alpha_p \sum_{j=1}^{m} N_j \prod_{k=1,\, j}^{m} (\nu_k - \lambda) \right] \tag{37}$$

and m is the number of multiple steady states of the single particle in isolation. Now Eq. 36 produces two kinds of eigenvalues of the operator L_N. The roots to the equation $\hat{p}_N(\lambda) = 0$ will lead to *all* distinct eigenvalues of the reactor operator L_N. The remaining part of Eq. 36,

$$\left[\prod_{j=1}^{m} (\nu_j - \lambda)^{(N_j - 1)}\right] = 0 \tag{38}$$

will produce multiple eigenvalues provided $N_j \geq 3$. The equation $\hat{p}_N(\lambda) = 0$ may be written as

$$\Phi(\lambda) = \Sigma(\lambda) \tag{39}$$

where we have identified the following two functions

$$\Phi(\lambda) \equiv \frac{(\lambda - \mu_N)}{\alpha_f \alpha_p} \tag{39a}$$

$$\Sigma(\lambda) \equiv \frac{N_1}{(\lambda - \nu_1)} + \frac{N_2}{(\lambda - \nu_2)} + \frac{N_3}{(\lambda - \nu_3)} \tag{39b}$$

somewhat analogously to the linear case earlier. This situation represents the general case where all the steady states are oc-

cupied with at least one particle (i.e., $N_k \neq 0$, $\forall k = 1, 2, 3$). Also, this is a nonuniform or patterned steady state since $\nu_1 \neq \nu_2 \neq \nu_3$. We will later illustrate the spectrum of the operator L_N for particular cases such as $N = 3$. Uniform solutions (which imply that $\nu_1 = \nu_2 = \nu_3 = \nu$) will also be considered in our analysis.

Stability of uniform stationary states

The characteristic equation for the uniform case is given by an equation equivalent to Eq. 14 with $(\alpha_p + \phi^2)$ replaced by ν_k ($k = 1, 2, 3$) for particular state we want to analyze. As before, we have a multiple root given by $\lambda_j = \nu_k$ ($k = 1, 2,$ or, 3), $j = 2, 3, \ldots, N$ for the case of $N \geq 3$. The other two extra roots ($j = 1$ and $N + 1$) are given by a quadratic equation that is similar to Eq. 16. In order to proceed further with the analysis we may use functions 39a and 39b conveniently specialized for the case of uniform solutions. The function $\Phi(\lambda)$ is given

$$\Phi(\lambda) = \frac{\lambda - \mu_N}{N\alpha_f\alpha_p} \tag{40a}$$

and the function $\Sigma(\lambda)$ is as follows

$$\Sigma(\lambda) = \frac{1}{(\lambda - \nu_k)}, \quad k = 1, 2, \text{ or } 3. \tag{40b}$$

Since the geometrical features of $\phi(\lambda)$ and $\Sigma(\lambda)$ are the same as those for the linear case, the location of the eigenvalues are determined as in Figure 1. Of course in the present case, the two curves may translate (with change in parameters) along the λ-axis to yield eigenvalues that can assume both positive and negative values.

Uniform solutions clearly exist for the assembly whether or not individuals in isolation exhibit multiplicity. We first discuss the stability of uniform solutions when single particles have unique (always stable) steady states, Figure 3.1a. As observed previously, collaborative multiplicity of uniform solutions may or may not exist depending on the choice of parameters. When there is only a unique steady state it is found to be stable until (with change is some parameter, say N or α_f) a bifurcation is reached leading to three steady states, Figure 6. The asymptotic stability criterion turns out to be

$$\frac{\mu_N}{N\alpha_f}\left[1 + \frac{1}{M_p} f'(\tilde{x})\right] \geq 1 \tag{41}$$

where $\tilde{x}$ is the steady state of each particle in the assembly. When there is multiplicity in the uniform steady state of the assembly $\tilde{x}$ can of course take on any of three different values. Denoting the intermediate steady state by particles all at state $\tilde{x}_I$, the "upper" one by particles at state $\tilde{x}_{II}$, and the "lower" one by particles at state $\tilde{x}_{III}$, their individual asymptotic stabilities are governed by the status of the inequality Eq. 41 with $\tilde{x}$ substituted by $\tilde{x}_I$, $\tilde{x}_{II}$, or $\tilde{x}_{III}$. Arce (1990) has shown that the uniform steady states corresponding to $\tilde{x}_{II}$ and $\tilde{x}_{III}$ are always stable while that corresponding to $\tilde{x}_I$ is always unstable. It is noteworthy here that the uniform pattern containing particles of steady state $\tilde{x}_I$ is unstable although the single particle will have been stable in isolation with the fluid. We will refer to this as *collaborative reversal of stability*.

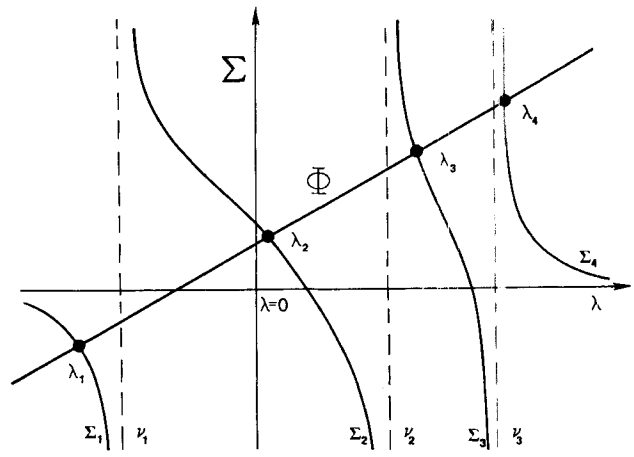

Figure 8. Geometrical view of spectrum of L_N (configuration 6) for three-particle problem.

Next, we discuss uniform stationary states that feature particles with multiple steady states in isolation, Figure 3b. Consider first the uniform steady state of the assembly with particles at the intermediate steady state (denoted earlier as "1" as in Figure 3b), and lie along branch 4 in Figure 5. As the steady state of the catalyst particle is unstable, the eigenvalue ν_1 of the single-particle operator must be negative. Since from Figure 1 (with ν_1 replacing ν for this case) the smallest eigenvalue λ_1 is less than ν_1, the negativity of ν_1 implies that of λ_1. Consequently, the uniform stationary state of the assemblage of all catalyst particles at the intermediate state "1" is always *unstable*. There is thus no collaborative reversal of instability.

We next consider uniform steady states in which *all* particles are at either steady state 2 or 3, Figure 3b, which lie along either branch 1 or 10 in Figure 5. The asymptotic stability criterion is given by Eq. 41 with $\tilde{x}$ replaced by either $\tilde{x}_2$ or $\tilde{x}_3$.

Condition 41 is seen to hold for a uniform steady state along a *particular branch* if there is only one such steady state on the branch. However, when two steady states occur on the branch then condition 41 is violated for one of them, thus producing again an instance of collaborative reversal of stability.

Stability of nonuniform (patterned) states

For any pattern k (see, for example, Figures 4 and 5 for the three-particle assembly) the distribution of eigenvalues may be either as shown in Figure 8 or as in Figure 9. Figure 8 represents a pattern that contains at least one particle at steady state 1 (at which it will be unstable in isolation with the fluid). Since $\nu_1 < 0$, the eigenvalue λ_1, which is necessarily less than ν_1, is also negative. Thus the pattern in question is always unstable. It is therefore noteworthy that no collaborative effort of particles with stable steady states (in isolation) can stabilize a pattern as long as there is at least one other particle in the unstable steady state. We may refer to this as the infeasibility of a collaborative reversal of instability.

Figure 9 features the eigenvalues for a pattern with particles that are stable in isolation either at steady state 2 or 3. The

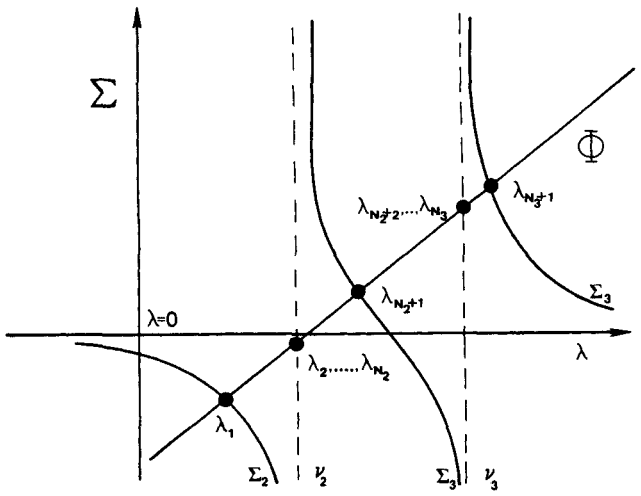

Figure 9. Geometrical view of spectrum for patterns showing particles in lower and upper stationary states of the individual catalyst particle only.

necessary and sufficient condition for asymptotic stability for pattern k (containing no particles with the unstable state 1) with N_2 particles in steady state 2 and N_3 particles in steady state 3 is found to be

$$\frac{\mu_N/\alpha_f}{N_2\left[1+\frac{f'(\tilde{x}_2)}{M_p}\right]^{-1}+N_3\left[1+\frac{f'(\tilde{x}_3)}{M_p}\right]^{-1}}\geq 1 \qquad (42)$$

At this point it is opportune to recall the issue of multiplicity along a pattern of the type in question. Where there is a unique steady state on the pattern (as when Eq. 31 does not hold) condition Eq. 42 is seen to hold (Arce, 1990). When condition Eq. 31 holds, then multiplicity occurs in the branch and one of the steady states is unstable because Eq. 42 is violated while for the other Eq. 42 holds, implying asymptotic stability of that pattern.

Conclusions

Particles in an assembly behave very differently with respect to *both* multiplicity and stability from single particles in isolation. Thus we have collaborative abatement or enhancement of multiplicity and collaborative reversal of stability of steady states in the particles. Collaborative reversal of instability cannot occur (unless possibly some external control measure is adopted). Collaboration here refers to mutual interaction between the particles jointly and the fluid.

The reversal effect on stability is of course attributed to the fact that the system does not permit the fluid to remain stable so that the particles (which would have been stable otherwise in the steady fluid) cannot be stable also. It should be noted that this phenomenon of reversal of stability occurs even for uniform solutions so that it is *not* an *exclusive property* associated with symmetry breaking.

The role of single-particle studies in determining reactor behavior is far more subtle than imagined before. The simple setting in this paper, although somewhat removed from that of an industrial reactor, has some definite implications to it. In any reactor, one could envisage, locally, a population of catalyst particles exposed to a particular fluid concentration. In this connection, the cell model that links several tanks such as the one analyzed in this paper is an interesting model to study in regard to the issues generated here.

We have been concerned with raising what we believe to be important phenomenological issues in reactor behavior. They point to the strong variability (due to the appearance of patterns) of the behavior of the reactor with respect to conversion and selectivity in multiple reaction systems. It is most important to note that we have retained only the models that have been in common use, introducing no additional attribute such as direct interaction between particles. All of the phenomena discussed in this paper arose from fluid-mediated interaction between particles alone. In unearthing them our analysis has exploited prior knowledge of the isolated single-particle problem to arrive at a simple characterization of the steady state multiplicity and stability of the reactor. When single-particle information is not available it is probable that a more direct approach in which use of the symmetry (permutation) group covariance of the original reactor equation to obtain the reduced bifurcation equations is more appropriate.

Acknowledgment

We are grateful to the School of Chemical Engineering of Purdue University for financial assistance and to the Purdue Research Foundation for a David Ross Fellowship to Pedro Arce, which made this research possible.

Notation

a_p = area of catalyst particle
A = solid-fluid interaction operator
B = fluid-solid interaction operator
c = molar concentration
Da = Damkhöler number
$D(x_f)$ = function, Eq. 23
$f(x_j)$ = nondimensional kinetic rate function
F = molar flow rate
F = fluid operator
$F(x)$ = function, defined before Eq. 27
$F^k(x_f)$ = function, Eq. 29
H = direct-sum Hilbert space
H_f = Hilbert space associated with fluid phase
H_p = Hilbert space associated with particle phase
I_N = unit matrix in H_p
$k(T)$ = kinetic constant
k_m = mass transfer coefficient
L_N = reactor operator in H
M_a = constant, defined before Eq. 29
M_m = maximum number of distinguishable branches given by Eq. 26
M_p = constant given by $M_p \equiv \alpha_p/Da$
$\mathbf{1}_N$ = unit vector in H_p
$r'(c_j)$ = kinetic reaction rate, Eq. 3
$r(x_j)$ = kinetic reaction rate, Eq. 7
S_N = particle phase operator
t = nondimensional time
t' = dimensional time
u_j, u_k = vectors in H_f
V = total volume of reactor
v_j, v_k = vectors in H_p
w_j, w_k = vectors in H
$\tilde{x}$ = nondimensional concentration of steady state value
$\underline{x}_f, \tilde{x}_f$ = nondimensional fluid concentration at bifurcation points of isolated particle

$\underline{x}_f^k$, $\tilde{x}_f^k$ = nondimensional solid concentration of kth branch at bifurcation points
$\underline{x}_p$, $\tilde{x}_p$ = nondimensional solid concentration at bifurcation points of isolated particle
x = vector of concentration values in H
$\hat{x}$ = perturbation vector of concentration values in H
x_N = vector of concentration values in H_p
$\bar{X}_N^k$ (x_f) = arithmetic mean, Eq. 24

Greek letters

α_f, α_p = nondimensional mass transfer coefficients
δ = self-adjoint parameter defined by $\delta \equiv \alpha_f/\alpha_p$
$\Sigma(\lambda)$ = function, Eq. 18b, 39b
ϵ = reactor void fraction
ϕ = Thiele modulus for first-order reactions
$\Phi(\lambda)$ = function, Eq. 18a or 39a
λ, λ_j = eigenvalues of operator L_N
μ_N = parameter defined by $\mu_n \equiv (1 + N\alpha_f)$
ν = eigenvalue of particle phase operator for linear case
ν_j, ν_k = eigenvalues of particle phase operator for linearized case
σ = adsorption, desorption constant
σ' = parameter defined by $\sigma' \equiv c_0\sigma$
θ_f = residence time of reactor

Subscripts

f = fluid
j = jth particle, jth eigenvalue of L_N
k = kth steady state, kth eigenvalue of L_N
N = number of particles
o = feed
p = particle

Superscript

k = kth steady state of system, branch of steady states

Inner products

$\langle , \rangle$ = inner product in H
$(,)_p$ = inner product in H_p

Literature Cited

Arce, P., and D. Ramkrishna, "Self-Adjoint Operator of Transport in Interacting Solid-Fluid Systems," *Chem. Eng. Sci.*, **41**, 1549 (1986).

Arce, P., "Pattern Formation and Particle-Reactor Instabilities in Heterogeneous Catalytic Reactors," Ph.D. Thesis Purdue Univ. (December 1990).

Brown, J., and R. Schmitz, "Multiplicity of States in Systems of Interacting Catalyst Particles," *Chem. Eng. Commun.*, **84**, 191 (1989).

DeVera, A., and A. Varma, "Substrate-Inhibited Enzyme Reaction in a Tubular Reactor with Axial Dispersion," *Chem. Eng. Sci.*, **34**, 275 (1979).

Do, D., and R. Rice, "Determination of the Condition for the Existence of Composition Minima in a CSTR via Spectral Analysis," *Chem. Eng. Sci.*, **40**, 291 (1985).

Gmitro, J. I., and L. E. Scriven, "A Physicochemical Basis for Pattern and Rhythm," *Intracellular Transport*, K. B. Warren, ed., Academic Press, New York (1966).

Golubitsky, M., I. N. Stewart, and D. G. Schaeffer, *Singularities and Groups in Bifurcation Theory*, **II**, Springer-Verlag, New York (1988).

Hegedus, L., S. Oh, and K. Baron, "Multiple Steady States in an Isothermal, Integral Reactor: The Catalytic Oxidation of Carbon Monoxide over Platinum-Alumina," *AIChE J.*, **23**, 632 (1977)

Liu, S., and N. R. Amundson, "Stability of Adiabatic Packed-Bed Reactors. An Elementary Treatment," *Ind. Eng. Chem. Fundam.*, **1**, 200 (1962).

Luss, D., "Uniqueness Criteria for Lumped and Distributed Parameter Chemically Reacting Systems," *Chem. Eng. Sci.*, **26**, 1713 (1971).

Luss, D., and N. R. Amundson, "Stability of Batch Catalytic Fluidized Beds," *AIChE J.*, **14**, 211 (1968).

Mankin, J. C., and J. L. Hudson, "The Dynamics of a Nonisothermal Catalyst Particles in a Surrounding Fluid," *AIChE J.*, **32**, 1208 (1986).

Othmer, H. G., and L. E. Scriven, "Instability and Dynamic Pattern in Cellular Networks," *J. Theor. Biol.*, **32**, 507 (1971).

Pismen, L., and I. Kharkats, "Asymmetric State of a Heterogeneous Exothermic Reaction," *Dokl. Akad. Nauk. SSR*, **178**, 901 (1968).

Ramkrishna, D. and N. Amundson, *Linear Operator Methods in Chemical Engineering with Applications to Transport and Chemical Reaction Systems*, Prentice-Hall, Englewood Cliffs, NJ (1985).

Ramkrishna, D., and P. Arce, "Self-Adjoint Operators of Transport in Interacting Solid-Fluid Systems. II," *Chem. Eng Sci.*, **43**, 933 (1988).

Ramkrishna, D., and P. Arce, "Can Pseudohomogeneous Reactor Models be Valid?" *Chem. Eng. Sci.*, **44**, 1949 (1989).

Sattinger, D., *Group Theoretic Methods in Bifurcation Theory*, Lecture Notes in Mathematics 762, Springer-Verlag, New York (1979).

Schmitz, R., and T. Tsotsis, "Spatially Patterned States in Systems of Interacting Catalyst Particles," *Chem. Eng. Sci.*, **38**, 1431 (1983).

Tsotsis, T., "Spatially-Patterned States in Systems of Interacting Lumped Reactors," *Chem. Eng. Sci.*, **38**, 701 (1983)

Manuscript received June 26, 1990, and revision received Nov. 27, 1990.